CCFE-PR(16)57

S. Murphy-Sugrue, J. Harrison, N. Walkden,P. Bryant, and
J. W. Bradley

# Particle-In-Cell Simulations of the Ball-Pen Probe

# Particle-In-Cell Simulations of the Ball-Pen Probe

S. Murphy-Sugrue[1,2], J. Harrison[1], N. Walkden[1], P. Bryant[2], J. W. Bradley[2]

***[1]Culham Centre for Fusion Energy, Culham Science Centre, Abingdon, Oxon, OX14 3DB, United Kingdom***
***[2]Department of Electrical Engineering and Electronics, University Of Liverpool, Brownlow Hill, Liverpool, L69 3GJ, United Kingdom***

Ball-pen probes have been deployed in the SOL of numerous magnetic confinement experiments to make direct measurements of the plasma potential. They have also been used simultaneously with Langmuir probes to make fast measurements of the electron temperature. Despite strong empirical evidence for the success of the BPP it lacks a theoretical underpinning of its collection mechanism. In this paper we investigate the capability of the probe to measure the plasma potential by means of Particle-In-Cell simulations using VSim [C. Nieter et al. J. Comp. Phys, 1, 196 (2004)]. The BPP is found to float at a potential offset from the plasma potential by a factor $T_e\alpha_{BPP}$. By simulating BPPs and Langmuir probes, excellent agreement has been found between the measured electron temperature and the specified source temperature. The transport mechanism for both ions and electrons has been determined. E x B drifts are observed to drive electrons and ions down the tunnel. This mechanism is sensitive to the diameter of the probe.

# Particle-In-Cell Simulations of the Ball-Pen Probe

S. Murphy-Sugrue[1,2], J. Harrison[1], N. Walkden[1],P. Bryant[2] J. W. Bradley[2]

November 1, 2016

## 1 Introduction

Measurements of the plasma potential ($\Phi$) and its fluctuations are vital for modelling transport phenomena in the edge region of tokamaks [1]. In theory the value of the plasma potential can be determined from the IV curve of a Langmuir probe. A simple expression [2] that relates the floating potential of the probe ($V_{LP}$) to the local plasma potential is

$$V_{LP} = \Phi - T_e \ln(R) \tag{1}$$

where $T_e$ is the electron temperature in eV and R the ratio of the electron saturation current($I^-_{sat}$) divided by the ion saturation current ($I^+_{sat}$). The logarithm of $R$ is often denoted as $\alpha$ such that

$$\alpha_{LP} = \ln(R) = \ln\left(\frac{I^-_{sat}}{I^+_{sat}}\right) \tag{2}$$

In principle it is possible to sweep the bias voltage across a Langmuir probe to derive $V_{LP}$, $T_e$ and $\alpha_{LP}$. The local plasma potential can then be obtained from equation 1. However in practice, especially in fusion plasmas, it is not possible to measure $R$. The high plasma density and temperature restricts the bias voltage that can safely be applied to the probe. Biasing the probe too close to the plasma potential would draw too high a current from the plasma and cause irreversible damage to the probe, it can also drain the flux tube, changing the plasma potential in the process. Another issue occurs

with determining the electron temperature from the IV curve. It is well documented that the electron temperature is often over-estimated using probe techniques in magnetised plasmas [3]. This would also lead to an error on the inferred value of the plasma potential. The ability to measure the plasma potential using DC measurements is desirable as a high time resolution is required to track the evolution of the potential between and during transient events such as filaments. The motion of filaments is strongly influenced by E x B drift effects [4]. Standard Langmuir probe measurements do not have the time resolution for studying potential evolution because the voltage has to be swept.

Various advanced probe techniques have been developed that aim to measure the plasma potential directly without needing an electron temperature measurement. These include emissive probes [5] and the Ball-Pen Probe (BPP) [6]. The emissive probe is not well suited to fusion plasmas as it requires a thin filament of wire to be exposed to the plasma making it structurally weak. The BPP is well suited to the tokamak edge as it is a robust diagnostic capable of surviving high heat loads [7]. The BPP will be the focus of this paper. Developed in 2004 [6] the BPP was designed to reduce the ratio of saturation currents to 1. If this can be achieved then $\alpha_{BPP} = 0$ and the probe will float at the plasma potential as evident from equation 1.

Despite empirical confirmation of the BPPs capabilities [1], [6],[8], [9] the probe is lacking a model based on first principles to confirm the collection mechanism. Presented in this paper are the results of 3D Particle-In-Cell simulations of the BPP design, previously employed on MAST, for a range of probe diameters and depths. The main aim of this study is to reproduce the experimental observations and determine if the BPP is capable of measuring the plasma potential. The paper will also investigate the capability of the BPP to make electron temperature measurements. These simulations were carried out using VSim [10]. In section 2 the design of the BPP and the theory of why it was designed this way is discussed. Section 3 summarises the results from experimental work that has been carried out with the BPP. The simulation model is introduced in section 4 followed by a description of the transport mechanism in section 5. The paper then moves on to explain the effects of probe diameter in section 6. The capability of the probe to measure the plasma potential and electron temperature is explored in sections 7 and 8 respectively. Section 9 details simulations carried out with a realistic ion mass. The effects of probe depth and temperature are explored in sections 10 and 11 respectively.

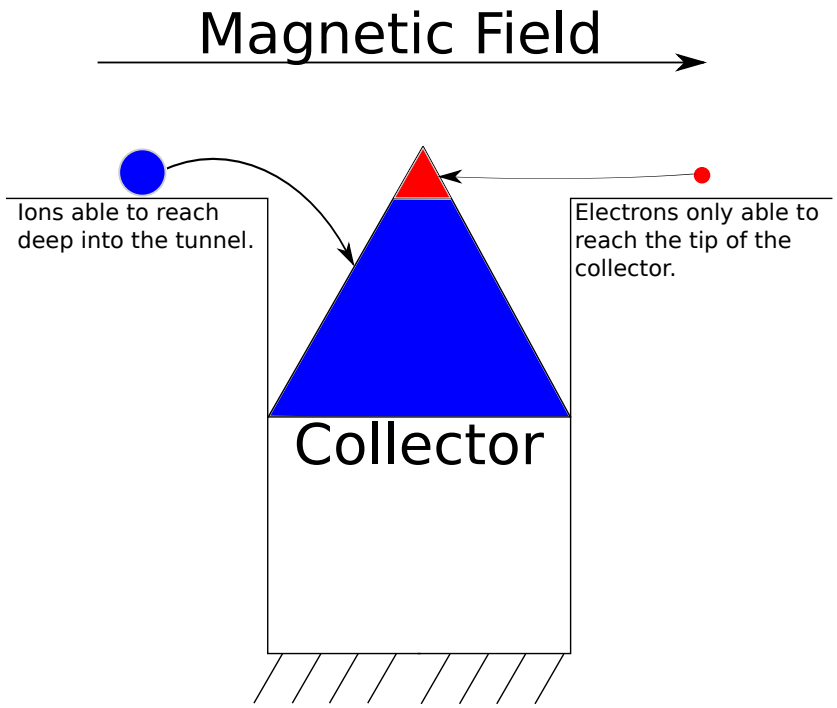


Figure 1: A schematic of the initial design of the BPP proposed by Adamek [6]. The probe is orientated such that the axis of the tunnel is perpendicular to the magnetic field.

## 2 The BPP Design and Theory

There are currently two designs for the BPP. The initial design [6] consisted of a conically shaped collector shielded by a tube of insulating boron nitride. This design is shown in figure 1. The probe is aligned such that the axis of the tunnel is near perpendicular to the magnetic field. The vertical position of the collector can be adjusted to alter the collection area that is exposed to the plasma. By recessing the collector inside the tunnel, the BPP aims to exploit the difference between the ion Larmor radius ($\rho_i$) and the electron Larmor radius ($\rho_e$). As shown in figure 1, electrons with their small gyro-orbits will only be able to access the small tip of the collector, with area ($A_e$), whereas the larger ion gyro-orbit allows them to enter deep into the tunnel and access a much larger collection area ($A_i$). The electrons have a much larger parallel current density ($J_e$) relative to that of the ions ($J_i$). It was

desired to achieve a value of $R = 1$. In order for this to occur the following criteria must be met

$$I_e = A_e J_E \quad = \quad I_i = A_i J_i \tag{3}$$

As $J_e > J_i$ it is only possible to achieve a value of $R = 1$ if $A_e < A_i$. This is the reason for varying the impact area for ions and electrons in Adamek's design. By adjusting the effective collection areas of the probe for the different species it was envisaged that an optimum recession depth would be found for which $R = 1$ [6]. In the ideal case it was thought that recessing the probe further than this height would result in more ions able to hit the probe than electrons leading to a value of $R < 1$ and a floating potential that was positive with respect to the plasma potential. Likewise, raising the probe above this optimum depth would lead to values of $R > 1$ as seen for a typical probe, in which case the probe would float negatively with respect to the plasma potential.

As will be detailed in section 3, both electron and ion currents are measured at the probe even when the collector is recessed beyond an ion Larmor radius. This was not predicted by the initial proposal for the collection mechanism. It has also been observed in experiments that the ratio $R$ falls approximately to unity once the probe is recessed beyond a few $\rho_e$ and does not vary significantly with further recession. These observations imply that particle transport to the probe is more complex and must occur perpendicular to the magnetic field. In [11] it was realised that because recession depth beyond a few $\rho_e$ did not affect probe readings, the conical shape of the collector was not necessary. Therefore a flat, cylindrical collector was then implemented and results compared favourably with the initial BPP conical design. Such a design was implemented in MAST [7], a schematic for which is shown in figure 2. The MAST BPP had a radius of 4 mm and a retraction depth of 5 mm. Adamek's conical probe had a radius of 4 mm and was operated with a variable retraction depth up to 2 mm.

# 3 Empirical Confirmation of the Ball-pen Probe Method

BPPs have been used to measure the plasma potential in multiple tokamak experiments including CASTOR[6], ASDEX Upgrade [1], COMPASS [8] and MAST [9]. They have also been employed in low-temperature magnetised

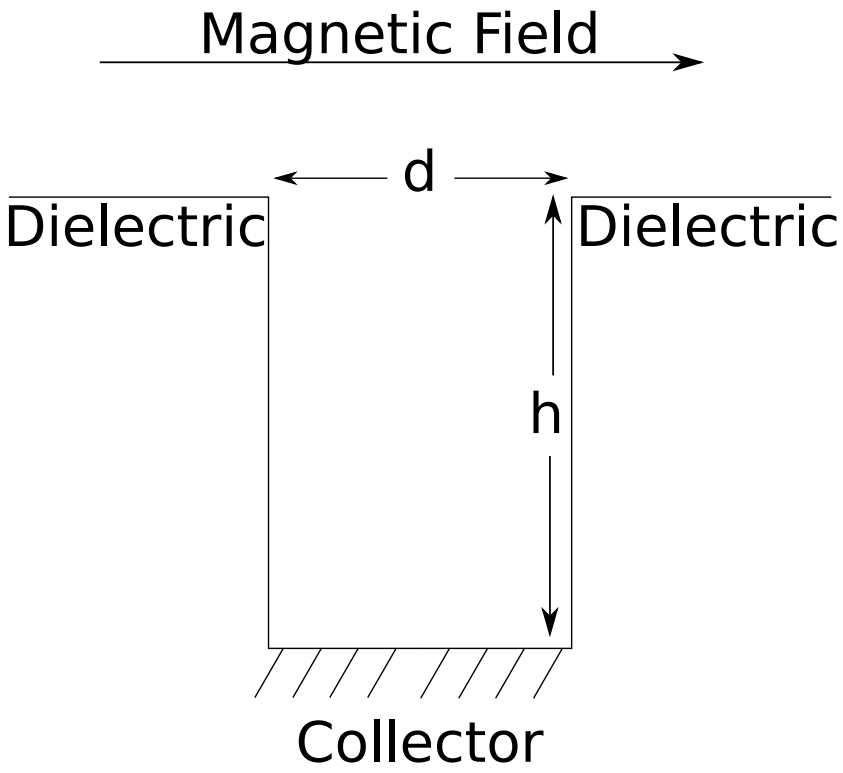


Figure 2: A BPP with a flat cylindrical collector. Also referred to as a Katsumata-type probe. $d$ is the diameter of the probe and $h$ the retraction depth. The BPP on MAST had a fixed retraction depth of 5 mm and a diameter of 4 mm

plasmas [12]. In Adamek's initial experiments an IV curve was produced by biasing the conical collector. This was repeated for various retraction depths, providing a measurement of the floating potential and $\alpha_{BPP}$ as as function of collector depth. It was found that at positive recession depths, which correspond to the collector located outside of the insulating tunnel, the probe behaved as a standard Langmuir probe and gave values of $\alpha_{BPP}$ that would be expected from probe theory. As the probe is recessed into the insulating tube $\alpha_{BPP}$ approaches zero, although it is never observed to actually reach zero. At a recession depth of $h = -0.5$ mm, corresponding to a recession depth of one ion Larmor radius, $\alpha_{BPP}$ was observed to reach a minimum of $\approx 0.2$ . At this point the probe floats at a potential which should be very close to the plasma potential according to equation 1. In further experiments almost identical measurements of the plasma potential were obtained using a BPP and a self-emitting Langmuir probe [13]. Comparative measurements of the plasma potential have also been made with the BPP and emissive probes [14]. Clearly there is strong empirical evidence for the success of the BPP technique however there are discrepancies between the experimental observations and the ideal theory. Firstly, $\alpha_{BPP}$ tends to zero but does not reach it, meaning there is always a higher electron current to the probe than ion current, even when the collector is recessed beyond multiple $\rho_i$. Ideal theory predicts negative values for $\alpha$ with sufficient probe recession which is not observed experimentally. As such, a model for particle transport to the collector is required to verify the experimental results.

2D PIC simulations of the BPP have been carried out by Komm [15]. In the simulations, the direction perpendicular to the magnetic field was neglected for ease of computation so that the probe essentially had infinite width in this direction. These simulations verified the suitability of equation 1 for the BPP. However values of $\alpha_{BPP} < 0$ were reported which have not been observed experimentally. This is in agreement with observations made from early 2D simulations carried out in VSim. It was found that when the direction perpendicular to the field was ignored, electrons could not reach the collector if it was recessed too far, suggesting that electric fields in the perpendicular direction were key to electron transport. Detailed 3D PIC modelling of the ion sensitive probe (ISP) has also been carried out by Komm [16]. The probe is of a similar design to the BPP but the probe head and tunnel are conducting and so biased to a set potential. It was found that a positive space charge region exists at the tunnel entrance as ions can penetrate deeper into the tunnel due to their large gyro-orbit. This leads to

an electric field across the tunnel entrance and subsequently an E x B drift is established that drives electrons and ions downwards into the tunnel. The reported transport mechanism is supported by experimental work carried out by Sullivan [17]. It is believed that a similar mechanism is also responsible for transport of electrons into the BPP tunnel but 3D PIC simulations are required to confirm this. We have carried out 3D particle-in-cell simulations of the BPP with a flat collector in order to explore the transport mechanism that allows electrons and ions to be collected. Simulations demonstrate the capability of perfect diagnostics within the constraints of Monte-Carlo noise. The plasma potential is known at each grid point and as the velocity of each particle is tracked, the electron temperature is also known. The simulations can therefore assess how well the BPP can reproduce input parameters of the simulation.

# 4 The Simulation Model

The simulations were carried out with the multi-dimensional PIC code VSim. The model is a full 3D simulation (3D3V) as earlier 2D simulations proved the BPP could not be modelled without taking all dimensions into account. The simulation domain models a region of the probe head, the entire BPP tunnel down to the collector and a region of plasma above the probe a few ion gyro-radii in depth in order to capture the magnetic presheath (MPS). The simulation domain is a cubic 3D Cartesian grid. The collector lies in the y-z plane at the bottom of the probe tunnel as illustrated in figure 3. At the beginning of the simulation the plasma region is filled with a quasi-neutral plasma, with velocities sampled from a Maxwellian distribution. The motion of individual particles is tracked as they move due to self-consistent electric fields and an imposed uniform magnetic field. Particles that hit the probe structure deposit their charge to that location and are then deleted from the system. A charge density and electrostatic potential evolve naturally, to a steady state, on the surface this way. Particles are injected along the top plane of the simulation at $x = 0$ to replenish those lost to the probe. The component of the velocity parallel to the magnetic field is sampled from the Emmert distribution [18]. The two perpendicular components are sampled from Maxwellian distributions. The y and z axis are periodic and the magnetic field makes an angle $\theta$ with the y-axis. The plasma potential is fixed at the top of the simulation to be 0 V.

| | |
|---|---|
| Magnetic field strength $B$ | 0.54T |
| Magnetic field inclination $\theta$ | $10°$ |
| Plasma density $n$ | $6.5 \times 10^{17}\, m^{-3}$ |
| Electron temperature $T_e$ | 60 eV |
| Ion temperature $T_i$ | 60 eV |
| Ion Larmor radius $\rho_i$ | 1 mm |
| Electron Mass $m_e$ | $9.11 \times 10^{-31}$ kg |
| Ion Mass $m_i$ | $900 m_e$ |
| Ion Charge $Z$ | $1.6 \times 10^{-19}$ C |

Table 1: Typical plasma parameters used in the simulations of the BPP.

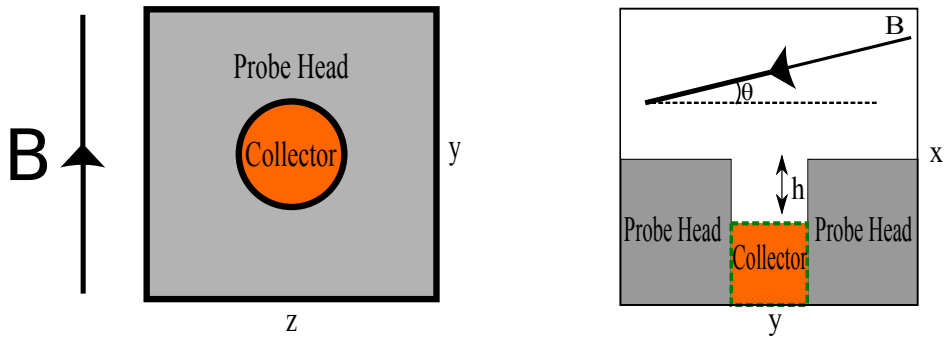


Figure 3: On the left - The BPP simulation domain as viewed from above looking along the x-axis. The collector sits at the bottom of the tunnel. On the right - A cross-section of the domain. $h$ is the recession depth.

## 4.1 Simulation Parameters

The plasma parameters able to be modelled in the simulations were restricted by computational demands. Typical simulated parameters are shown in table 1. These values are close to those found in the SOL of MAST however the simulated density is an order of magnitude less than the true density. Each grid cell in the PIC simulation must be smaller than a Debye length. Increasing the density, reduces the required grid spacing and so more grid cells are needed to simulate the same spatial region. Simulations were carried out with an increased density of $n = 1.0 \times 10^{18}\, m^{-3}$ which is more in line with MAST's conditions. The increased density did not appear to affect simulation results.

In experiments the BPP is aligned with respect to the magnetic field such that the axis of the probe tunnel is perpendicular to the field. In our simulations an angle $\theta$ was introduced as this was necessary for the particle injection algorithm. However a crude attempt at particle injection for the case of a perpendicular field was made in which particles were re-injected into the top of the simulation domain at the rate at which they were lost to the absorbing surfaces in the simulation. In this set-up it was found that the top surface of the probe-head floated positively with respect to the plasma potential as the ions were the more mobile species due to their large Larmor orbit. The mechanism for the BPP was then invalidated as recessing the probe would only further inhibit the electrons forcing the probe to float even more positively. However in a physical experiment the alignment of the probe will never be perfectly perpendicular to the magnetic field. A slight misalignment will allow electrons to stream along field lines to the surface, causing that surface to float negatively with respect to the plasma potential. The results discussed below are for a field alignment value of $\theta = 10°$.

In our simulations there are no collisions between the charged particles. The mean-free path ($\lambda$) for both electrons and ions is calculated to far exceed the length of the simulation domain ($\approx$ 5 mm) for the plasma parameters. From Wesson [19], using the stated simulated plasma parameters, $\lambda_{electron} =$ 7.2 cm and $\lambda_{ion} = 10$ cm. As a result particles can travel across the entire simulation domain multiple times without experiencing a collision. It has also been assumed that there are no neutrals or impurities present so the plasma consists of electrons and singly charged ions. Plasma-surface interaction effects such as secondary electron emission and sputtering have also been neglected.

# 5 Transport Mechanism

Experiments [6] and our simulations find that both electrons and ions are able to reach the collector even when it is recessed beyond $2\rho_i$. This observation can only be explained by some form of cross-field transport mechanism that drives particles down the tunnel. In the bulk plasma particles are born at the top of the domain and travel along field lines towards the probe. If they are in the right position and at a suitable phase of their orbit particles will enter the tunnel as shown in figure 4.

The orbits of the ions take them deep into the right side of the probe.

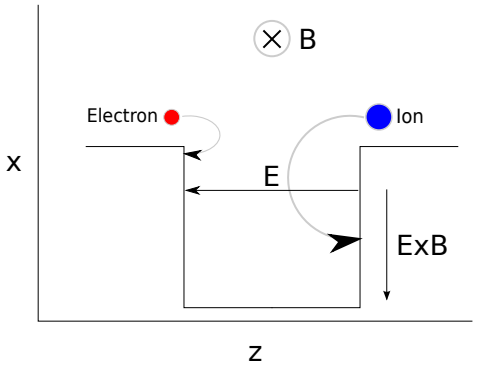


Figure 4: Electrons and ions orbit in opposite directions. Orbit of the ions takes them deep into the right hand side of the probe.

This results in an electric field across the tunnel of the probe in the negative z direction. The potential structure within the probe tunnel and the resulting electric field can be seen in figure 5. The interaction between the electric field in the z direction and magnetic field in the y direction results in an E x B drift that drives particles down the x-axis to the collector. Although the driving mechanism for the cross-field transport is the same for both species their exact trajectories down the tunnel are very different. Once in the tunnel particles will still continue to travel parallel to the field lines (along the y-axis) towards the tunnel wall. If a particle comes into contact with the tunnel wall it deposits it's charge there and is lost from the simulation. It is therefore unable to contribute current to the probe. In terms of motion parallel to the field electrons are the more mobile species due to their low mass. As a result a sheath forms in front of the floating tunnel wall to retard the flow of electrons to the wall. Only the most energetic electrons will be able to overcome this sheath potential to hit the wall. The less energetic electrons will reflect off the sheath and travel towards the other side of the tunnel. At the same time the electrons are driven down the tunnel due to the E x B drift. As a result the electrons follow a zig-zag path down the tunnel. The most energetic electrons are lost at the top of the tunnel as they are able to overcome the sheath potential. Therefore a less negative potential is required to maintain floating conditions further down the tunnel. The sheath potential on the wall becomes less negative with depth varying from -200 V at the top of the tunnel to -140 V at the bottom. As a result more and more

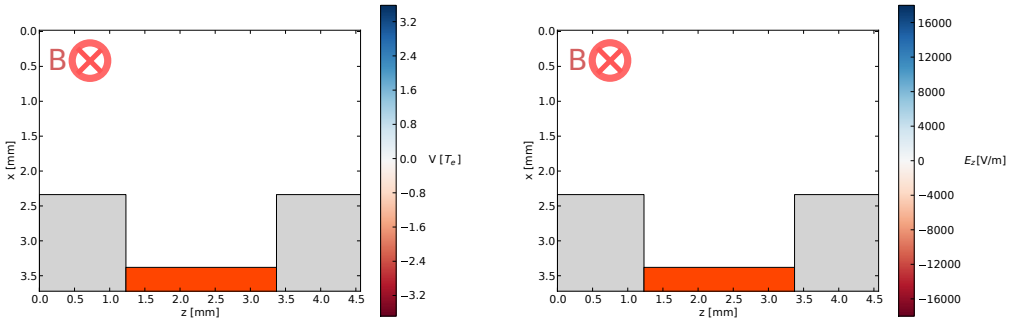


Figure 5: On the left - Cross section of the electric potential. On the right - Cross section of the resulting electric field in the z direction. $h = 1.1$ mm.

of the electron population is lost to the walls with only the least energetic not capable of overcoming progressively weaker sheath potentials to make it to the bottom of the probe. The parallel velocity distribution of electrons at the top and bottom of the tunnel is shown in figure 6. The width of the distribution narrows deeper into the tunnel as the high energy electrons are lost to the wall. The trajectory of an electron, taken directly from the simulation, that makes it all the way down to the probe is shown in figure 7. The gradient in potential along the wall results in an electric field in the negative x-direction. Both sides of the wall, perpendicular to the magnetic field see this potential drop. As electrons approach one side of the wall the resulting E x B drift will drive them to the left of the tunnel. It is not clear that this drift will impact probe measurements provided the collector area fills the collector tunnel as it does in the simulations.

The sheath acts to accelerate ions towards the wall so any ions that enter the sheath will be lost to the walls and unable to make it to the probe. Once entering the tunnel, an ion will continue its orbit around the field line whilst travelling parallel to the field towards the wall. To be collected an ion must have sufficient perpendicular velocity to make it to the probe before it's parallel velocity takes it to the wall i.e.

$$\left(\frac{h}{v_\perp}\right) < \left(\frac{d}{v_\parallel}\right) \tag{4}$$

where $h$ is the recession depth of the probe and $d$ the diameter. Ions that are collected by the probe have a higher perpendicular energy than parallel

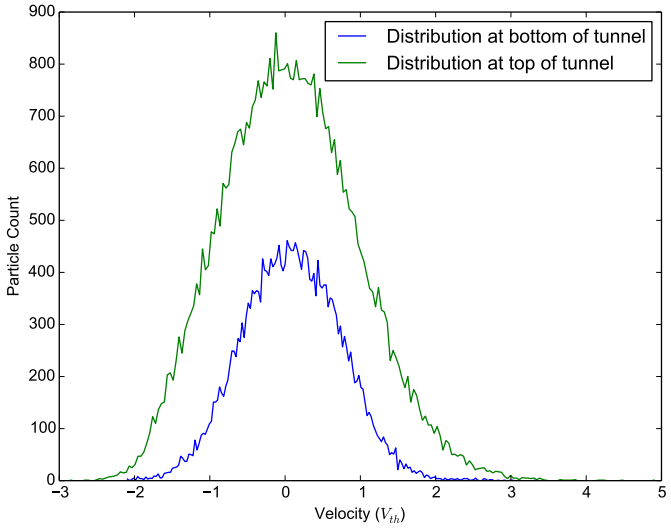


Figure 6: The parallel velocity distribution for electrons at the top and bottom ($h = 1.1$ mm) of the BPP tunnel. The distribution narrows deep into the probe as the more energetic electrons are able to overcome the sheath potential and hit the wall.

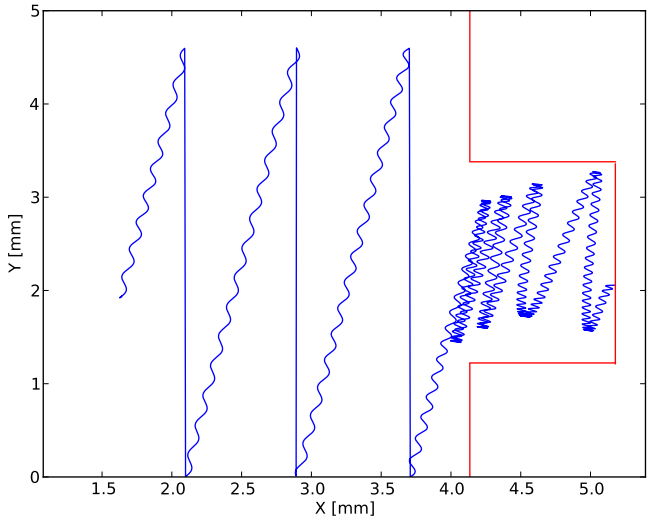


Figure 7: The electron trajectory in the x-y plane is shown in blue. Red lines show the walls of the probe. The electron follows the field across the periodic simulation domain until it enters the tunnel. Once in the tunnel the electron reflects back and forth due to sheath potential. Vertical lines represent the electron leaving the simulation on one side of the periodic boundary and re-emerging on the other side. $h = 1.1$ mm.

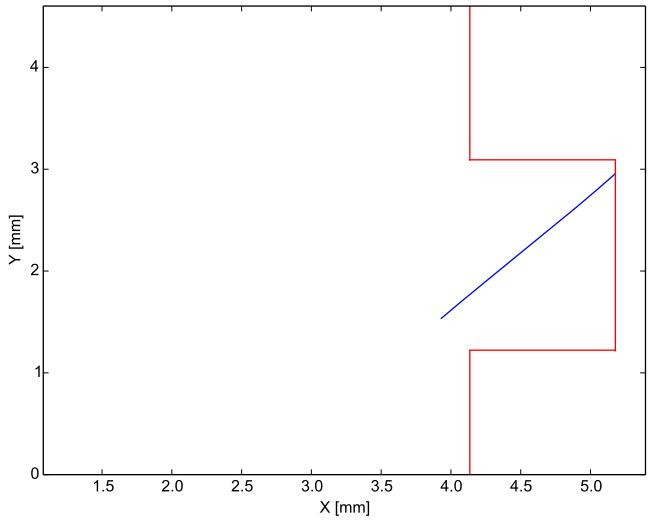


Figure 8: The trajectory of an ion as it enters the tunnel in the x-y plane is shown in blue. Red lines show the walls of the probe. The ion continues it's parallel motion along the field whilst its orbit perpendicular to the field takes it to the collector. The ion is able to make it to the collector before its parallel motion bring it to the wall.

energy when they enter the tunnel. Their perpendicular speed is increased in the tunnel due to the E x B drift. The Larmor radius of the ion must also be sufficiently large so that the ion can reach the collector i.e.

$$\rho_i \geq h \tag{5}$$

The trajectory of an ion that makes it to the probe is shown in figure 8.

The collection mechanism suggests that the proportion of the electron population that can make it to the probe should not be sensitive to the probe diameter. The electron parallel velocity will always exceed the E x B drift velocity so electrons will encounter the wall sheath multiple times before they are able to drift to the collector. On the other hand, the ions should be sensitive to the probe diameter. If the probe is too narrow ions will not have time to complete enough of their orbit to make it to the collector before encountering a tunnel wall. The tunnel must be sufficiently wide in

the parallel direction so as not to hinder the collection of the ions. This is investigated in section 6.

# 6 Effects of Probe Diameter

In order to investigate the effects of probe diameter, three probes with the same depth but different width were simulated. The diameters were a) 1.08 mm, b) 2.16 mm and c) 3.24 mm. Each probe had a depth of 1.04 mm. The ion Larmor radius in the simulations was $\rho_i = 1.02$ mm. For each probe diameter three simulations were carried out. One with the probe operating in floating mode and two biased cases where the collector was in ion collection and electron collection mode. The results for the floating potential are shown in figure 9 along with the measured value of R. The ratios presented were obtained using only one saturation current for each species. It has been observed in both simulations and experiments that the currents do not saturate, they instead increase linearly with applied bias voltage. This is discussed further in section 7. A linear interpolation has not been carried out so the true value of R is not known. The values are presented here as they demonstrate the effects of probe diameter even if their absolute value is not correct.

With increasing width a lower ratio R and a less negative value for $V_{BPP}$ is observed. The current collected per unit area for each species is shown in table 2. Beginning with the ions we find the current per unit area increases as the diameter increases. This is consistent with the collection mechanism, with a wider probe, ions have more time to make it to the probe before their parallel motion brings them to a tunnel wall. Increasing the diameter allows a higher proportion of the ion population to make it to the probe. The electron current remains fairly constant whilst increasing the probe diameter. There is actually a slight decrease in the current per unit area as the probe is made larger. The reason for this can be seen in figure 9. As the probe becomes wider, the plasma potential outside the probe tunnel increases as ions have a larger area to drift into and form a positive space charge region. All probes were biased to the same potential so this means the wider probes are biased less positively with respect to the plasma potential during electron collection. As a result they collect less electron current as it has not fully saturated at this collection voltage.

Due to computational demands the probes simulated are narrower than

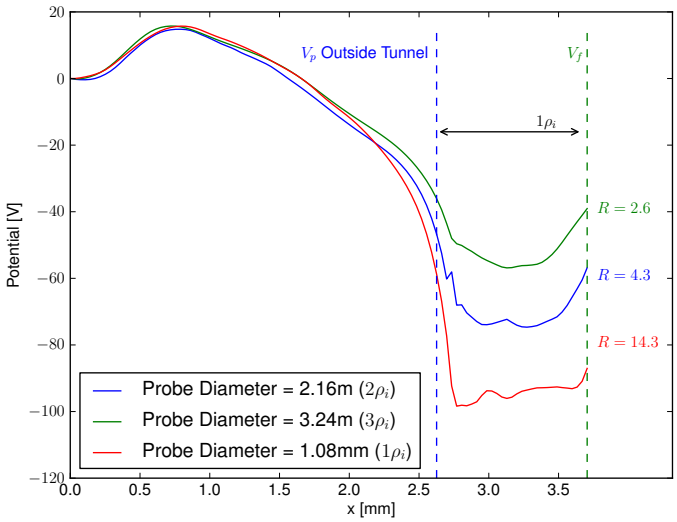


Figure 9: The potential structure across the simulation domain. The floating potential of the probe varies with tunnel diameter as does the value of R. The potential structure near $x = 0$ is a result of the source sheath, an artefact of particle injection in this region.

Table 2: The normalised current per unit area for probes of different diameters. A) 1.08 mm, B) 2.16 mm and C) 3.24 mm. The current is normalised to the current collected by the 1.08 mm diameter probe.

| Case | $I^+$ | $I^-$ | R |
|---|---|---|---|
| A | 1.0 | 1.0 | 14.3 |
| B | 2.7 | 0.9 | 4.3 |
| C | 3.9 | 0.7 | 2.6 |

probes typically employed on tokamaks. To the authors knowledge an experimental comparison of the influence of probe diameter on the value $R$ has not been reported. However in [20] three BPPs of the same design as MAST's were placed into the edge region of CASTOR to make simultaneous measurements of the plasma potential. The probes were of different diameter 1 mm, 2 mm and 4 mm. The authors concluded that the diameter was not a critical construction parameter but differences in the value of the measured plasma potential were observed. Values for $R$ were not reported. Differences in the plasma potential measurements were attributed to a misalignment of the probes with the magnetic surfaces. However in the region of minimal poloidal curvature, where the misalignment was lowest, it was found that the floating potential of the probe increased with probe diameter. The differences in potential measured in experiment were not as extreme as the differences found in the simulations. However the experimental electron temperature was estimated to be at 20 eV which is lower than the 60 eV electrons in the simulation. If the floating potential of the probe is changing that would suggest the value of $R$ also changes with probe diameter. This would be in agreement with the proposed transport mechanism.

# 7 Does the probe measure the true plasma potential?

In order to test the capability of the BPP to measure the plasma potential a range of simulations were carried out for probes of different sizes. For each probe, a simulation was carried out in which the probe was operated in floating mode in order to determine the floating potential of the BPP ($V_{BPP}$). Further simulations were carried out in order to determine $R$ and $\alpha_{BPP}$. In these simulations the probe was biased positively and negatively with respect to the plasma potential in order to determine a value for $I^-_{sat}$ and $I^+_{sat}$ respectively. It was observed that the currents for both species did not saturate. This behaviour has also been observed in experiments [21]. Following the method of [21] it was necessary to carry out further simulations with different probe bias voltages. The currents obtained at each voltage could then be extrapolated to obtain the value of $R$ at the plasma potential. Shown in figure 10 are four values for the ion current and electron current at different bias voltages for a probe with a diameter of 3 mm.

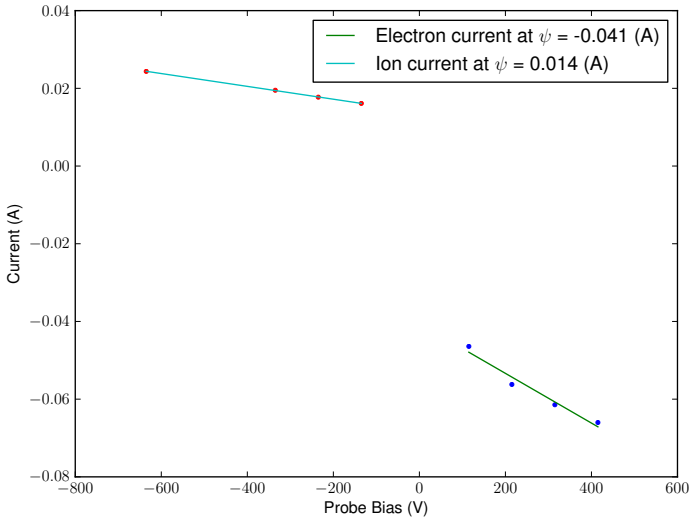


Figure 10: The current collected by the probe increases with probe bias. Linear interpolation was used to determine a value for each current at the plasma potential (0 V).

These currents increase linearly with probe bias, therefore it was possible to determine a value for $R$ by linearly interpolating both currents back to the plasma potential and defining their saturation values to be at this point. The values for the currents give $R = 3.02$ corresponding to a value $\alpha_{BPP} = 1.1$. These values are higher than what is typically observed in experiments where $\alpha_{BPP}$ is in the range

$$\alpha_{BPP} = 0.6 \pm 0.3 \tag{6}$$

However it is only for probes that are at least 4 mm in diameter that experimental measurements of $R$ have been reported. As demonstrated in section 6 a larger probe size reduces $R$ closer to that measured in experiments. Nevertheless if it can be demonstrated that the BPP floats at a potential offset from the true plasma potential by the product of $T_e\alpha$ then the BPP mechanism will be validated.

Shown in figure 11 is a plot of the potential across the simulation domain along the x-axis. The potential at each point represents the average potential across a circular cross-section centered over the BPP collector. The plasma potential is defined as the value at the top of the domain, where the profile is flat before the magnetic presheath (MPS) potential drop. The probe is found to float at a potential of $-69$ V relative to plasma potential. Based on the values of $\alpha_{BPP}$ extrapolated from figure 10 and $T_e = 60$ eV, equation 1 predicts the plasma potential should be $-3.8$ V. This is very close to the actual value for the plasma potential (0 V). The BPP will therefore float at a potential offset from the true plasma potential by a factor of $T_e\alpha_{BPP}$. An $\alpha_{BPP} = 0$ would be required for the BPP to truly float at the plasma potential.

# 8 Can the probe be used to make Temperature measurements?

Ball-pen probes have been used in conjunction with standard probes to make fast measurements of the electron temperature on multiple tokamak experiments and yielded excellent agreement with Thomson scattering data [22], [9]. The floating potential as measured by a BPP and LP can be written as

$$V_{BPP} = \Phi - \alpha_{BPP}T_e \tag{7}$$

$$V_{LP} = \Phi - \alpha_{LP}T_e \tag{8}$$

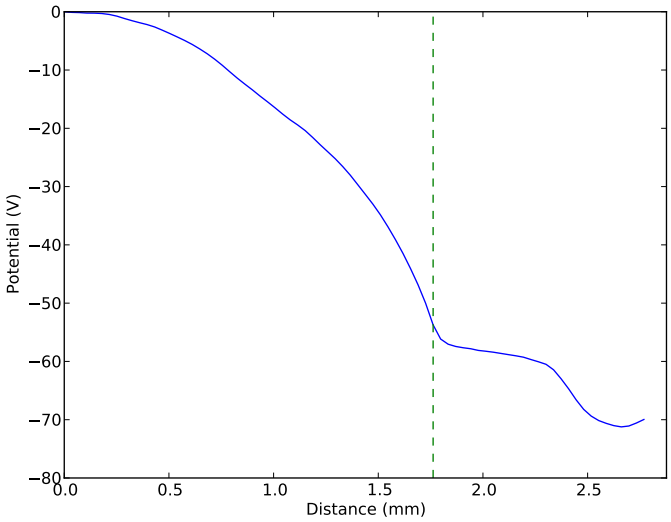


Figure 11: The plasma potential across the simulation domain, the dashed line shows the location of the BPP tunnel entrance.

By rearranging these expressions we obtain

$$T_e = \frac{V_{BPP} - V_{LP}}{\alpha_{LP} - \alpha_{BPP}} \tag{9}$$

For a planar Langmuir probe $\alpha$ is given by

$$\alpha = -\frac{1}{2} \ln \left( 2\pi \frac{m_e}{m_i} \left( 1 + \frac{T_i}{T_e} \right) \right) \tag{10}$$

So for a hydrogen plasma $\alpha_{LP} \approx 2.5$. It is not possible to measure this quantity in most tokamak experiments as the probe drains too high a current in electron collection mode and so the theoretical value must be used. $\alpha_{BPP}$ on the other hand can be measured directly in experiments as the currents to the collector are much lower. It is possible to use these two values along with a Langmuir probe and BPP operated in floating mode to determine $T_e$. All that is needed is a floating potential measurement from each probe, which can be made instantaneously and is only limited by the speed of the data acquisition system. In fusion plasmas $T_e$ is typically measured by sweeping a standard

Langmuir probe from ion collection to floating potential and then fitting an exponential to the IV curve. This method is slow relative to the BPP-LP method due to the time it takes to sweep the probe voltage. The BPP-LP method then offers better time resolution and potentially more accurate measurements of $T_e$ as it uses a floating potential measurement from the Langmuir probe which is considered to be in the safe region of the IV curve for a probe in magnetised plasma [23].

Additional simulations were carried out in order to test the capability of the BPP-LP pair to make electron temperature measurements. The BPP was replaced with a flush-mounted probe (FMP) and operated in floating mode to obtain $V_{LP}$. As discussed previously in section 7, $\alpha_{BPP}$ and $V_{BPP}$ have already been measured. As in experiments our simulations are not capable of measuring $\alpha_{LP}$. In magnetised plasma the collection length of the probe operating in electron collection mode can extend very far into the plasma. It is not possible to capture this region in our simulation domain and so it is not possible to collect $I^-_{sat}$. Following experimental procedure we will therefore use the theoretical value for $\alpha_{LP}$ provided by equation 10.

As before, results are stated for the $3mm$ diameter probe with an electron temperature of $60eV$. The FMP is found to float at a potential $V_{LP} = -129$ V. Combining this with $\alpha_{BPP} = 1.1$, $V_{BPP} = -69$ V and the theoretical value of $\alpha_{LP} = 2.14$ for the reduced ion mass we obtain a value of $T_e = 58.3$ eV which is in very good agreement with the specified temperature. This method is a viable way of making fast electron temperature measurements provided $\alpha_{BPP}$ is known. The measurement of $T_e$ can be combined with $V_{BPP}$ to determine the true plasma potential.

# 9 Simulations with Realistic Ion Mass

Simulations were carried out with an ion mass equal to the proton mass in order to allow a direct comparison with experiments. The probe size was also increased to a diameter of 4 mm, the same as that used by Adamek in his original paper [6]. This required the entire simulation domain to be expanded in the y and z dimensions which required more computer cores to run. 64 cores were required for these simulations, a fourfold increase. The simulated magnetic field strength was set to 1.3 T equivalent to the field strength used in Adamek's experiments. The collector depth was fixed to 1 mm. Three runs were carried out where the probe was biased at different

voltages, so that an extrapolation could be carried out to determine $R$ and a floating run was completed to determine $V_{BPP}$. The values found for these quantities are

$$R = 2.8 \quad \alpha_{BPP} = 1.04 \quad V_{BPP} = -67.6V \tag{11}$$

Which are in good agreement with equation 1. The value for $\alpha_{BPP}$ obtained in the simulations sits outside the accepted range derived from experiments for a probe of this size given in equation 6. This range is obtained using conical collectors where as the simulated probe was flat. In the experiment described in section 6 where three flat collector probes of different diameter were used simultaneously to measure the plasma potential, a 2mm BPP with a conically shaped collector was also used for comparison with the flat collectors. Out of the four probes, the 2mm conical BPP was consistently found to float at the highest potential. This would suggest a smaller diameter conical BPP can achieve the same ratio $R$ as a larger, flat collector BPP. This result could shed light on why the probes with a flat collector that have been simulated measure a higher $R$ than the conical BPPs whose experimental values of $R$ have been reported. This does not effect the capability of either probe to make plasma potential or electron temperature measurements, provided $\alpha_{BPP}$ is known for the probe that is employed.

# 10 Effects of Probe Depth

In Adamek's experiment [6] it was found that the value of R reached a minimum when the probe was recessed 0.5mm equivalent to $1\rho_i$. Once the probe was recessed beyond this depth the value of R increased. Simulations have also detected this sensitivity. Both electron and ion currents to the probe decrease as the probe is recessed deeper into the tunnel, as more particles are absorbed by the tunnel walls. However the electron current is slow to fall off as electrons can carry on reflecting off the sheath while being driven towards the collector by E x B drifts. The reduced electron current is a result of the fact that the potential on the tunnel wall decreases with depth, i.e. becomes closer to the plasma potential. As a result gradually less of the electron population will be reflected by the weaker sheath potential. Increasing the probe depth makes it more likely that an ion's parallel velocity will take it into a tunnel wall before it can make it down to the collector. Ions are not able to reflect off the sheath and so the ion current declines at a faster rate than the

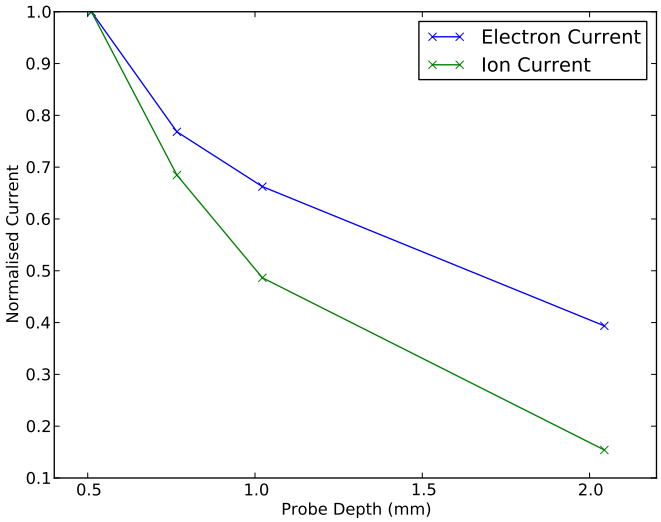


Figure 12: Normalised currents as a function of depth. The ion current falls off more quickly than the electron current. Each current is normalised to the first current from that species.

electron current therefore the value of R increases. It appears that as long as the BPP is recessed beyond a few $\rho_e$ the electrons become magnetically shielded and can only access the collector with E x B drifts. The probe then operates as a BPP. As long as this criteria is met and the probe depth is fixed with known $\alpha_{BPP}$ the probe depth is not an important parameter.

# 11 Effects of Temperature

Additional simulations were carried out with an increased electron and ion temperature of 120eV to determine if particle temperature had an impact on $\alpha_{BPP}$. As before, multiple simulations were carried out for different probe bias voltages so that $\alpha_{BPP}$ could be measured by interpolating the currents. For these runs, a value of $\alpha_{BPP} = 1.38$ was observed which is only a slight increase on the 60eV value ($\alpha_{BPP} = 1.1$). It does not appear that the temperature particularly effects the workings of the BPP. Though this investigation was not systematic and warrants further investigation in the future.

# 12 Conclusions

3D PIC simulations have verified that the BPP measures a potential offset from the true plasma potential by a factor $T_e\alpha_{BPP}$. BPPs in practice have obtained values as low as $\alpha_{BPP} = 0.6$. For electron temperatures on the order of 10 eV the difference between the floating potential of the probe and the true plasma potential will then be several volts. By simulating both a LP and a BPP the source temperature for the electrons was recovered validating the BPP-LP method for making fast electron temperature measurements.

The mechanism that allows electrons to reach the collector even when it is recessed far beyond their gyro-orbit has been confirmed. Inside the tunnel, electrons travel back and forth along field lines, reflected by the wall sheaths, whilst simultaneously undergoing E x B drifts. This mechanism suggests probe diameter could be an important construction parameter. Experimental measurements are needed to verify this. Probe depth is not an important constraint provided the collector is recessed sufficiently such that the electrons are magnetically shielded from the collector. A few $\rho_e$ is sufficient. An IV curve should be obtained for a probe before it is used in order to determine $\alpha_{BPP}$. Once this value is acquired it is then possible to use the BPP to extract the electron temperature and plasma potential.

# 13 Acknowledgements

This project has received funding from the European Unions Horizon 2020 research and innovation programme under grant agreement number 633053 and from the RCUK Energy Programme [grant number EP/I501045]. To obtain further information on the data and models underlying this paper please contact PublicationsManager@ccfe.ac.uk*. The views and opinions expressed herein do not necessarily reflect those of the European Commission. This work made use of the facilities of N8 HPC Centre of Excellence, provided and funded by the N8 consortium and EPSRC (Grant No.EP/K000225/1). The Centre is co-ordinated by the Universities of Leeds and Manchester. This work was supported by the Engineering and Physical Sciences Research Council [EP/K504178/1]

# 14 References

# References


[1] J. Adámek, V. Rohde, H.W. Müller, A. Herrmann, C. Ionita, R. Schrittwieser, F. Mehlmann, J. Stckel, J. Horacek, J. Brotankova, and ASDEX Upgrade Team. Direct measurements of the plasma potential in ELMy h-mode plasma with ball-pen probes on ASDEX upgrade tokamak. *J. Nucl. Mater.*, 390 391:1114 – 1117, (2009).

[2] P. C. Stangeby. Plasma diagnostics. 2(9):157, 1988.

[3] G F Matthews. Tokamak plasma diagnosis by electrical probes. *Plasma Physics and Controlled Fusion*, 36(10):1595, 1994.

[4] D. A. DIppolito, J. R. Myra, and S. J. Zweben. Convective transport by intermittent blob-filaments: Comparison of theory and experiment. *Physics of Plasmas*, 18(6), 2011.

[5] Roman Schrittwieser, JirAdmek, Petru Balan, Martin Hron, Codrina Ionita, Karel Jakubka, Ladislav Kryska, Emilio Martines, Jan Stckel, Milan Tichy, and Guido Van Oost. Measurements with an emissive probe in the castor tokamak. *Plasma Physics and Controlled Fusion*, 44(5):567, 2002.

[6] J. Adámek, J. Stöckel, M. Hron, J. Ryszawy, M. Tichý, R. Schrittwieser, C. Ionită, P. Balan, E. Martines, and G. Van Oost. A novel approach to direct measurement of the plasma potential. *Czechoslovak Journal of Physics*, 54(3):C95–C99.

[7] Walkden N.R 2014. Properties of intermittent transport in the mega ampere spherical tokamak. *PhD Thesis*, University of York(2014).

[8] R Pánek, J Adámek, M Aftanas, P Bílková, P Böhm, F Brochard, P Cahyna, J Cavalier, R Dejarnac, M Dimitrova, O Grover, and J Harrison et al. Status of the compass tokamak and characterization of the first h-mode. *Plasma Phys Contr F*, 58(1):014015, 2016.

[9] N. R. Walkden, J. Adámek, S. Allan, B. D. Dudson, S. Elmore, G. Fishpool, J. Harrison, A. Kirk, and M. Komm. Profile measurements in the

plasma edge of mega amp spherical tokamak using a ball pen probe. *Review of Scientific Instruments*, 86(2):023510, 2015.

[10] C. Nieter and J. R. Cary. Vorpal: a versatile plasma simulation code. *J. Comp. Phys*, 196(1):448–472, 2004.

[11] R. Schrittwieser, C. Ionitá, J. Adámek, J. Stöckel, J. Brotánková, E. Martines, G. Popa, C. Costin, L. van de Peppel, and G. van Oost. Direct measurements of the plasma potential by katsumata-type probes. *Czechoslovak Journal of Physics*, 56(2):B145–B150, 2006.

[12] J. Admek, M. Peterka, T. Gyergyek, P. Kudrna, M. Ramisch, U. Stroth, J. Cavalier, and M. Tich. Application of the ball-pen probe in two low-temperature mag-netised plasma devices and in torsatron tj-k. *Contributions to Plasma Physics*, 53(1):39–44, 2013.

[13] J. Adámek, J. Horacek, J. Seidl, H. W. Müller, R. Schrittwieser, F. Mehlmann, P. Vondracek, S. Ptak, COMPASS Team, and ASDEX Upgrade Team. Direct Plasma Potential Measurements by Ball-Pen Probe and Self-Emitting Langmuir Probe on COMPASS and ASDEX Upgrade. *Contrib Plasm Phys*, 54(3):279–284, 2014.

[14] J. Adámek, J. Stöckel, I. Ďuran, M. Hron, R. Pánek, M. Tichý, R. Schrittwieser, C. Ionit, P. Balan, E. Martines, and G. Oost. Comparative measurements of the plasma potential with the ball-pen and emissive probes on the castor tokamak. 55(3):235–242.

[15] M. Komm, J. Adamek, Z. Pekarek, and R. Panek. Particle-in-cell simulations of the ball-pen probe. *Contributions to Plasma Physics*, 50(9):814–818, 2010.

[16] M Komm, J Adámek, R Dejarnac, J P Gunn, and Z Pekarek. Transport of electrons in the tunnel of an ion sensitive probe. *Plasma Phys Contr F*, 53(1):015005, 2011.

[17] R.M. Sullivan, R. Ochoukov, and D.G. Whyte. Internal physics of the ion-sensitive probe. *Journal of Nuclear Materials*, 438, Supplement:S1253 – S1256, 2013. Proceedings of the 20th International Conference on Plasma-Surface Interactions in Controlled Fusion Devices.

[18] G A Emmert, R M Wieland, A T Mense, and J N Davidson. Electric sheath and presheath in a collisionless, finite ion temperature plasma. *Physics of Fluids*, 23(4), 1980.

[19] John. Wesson and J. W. Connor. *Tokamaks / John Wesson ; with contributions from J.W. Connor ... [et al.].* Clarendon Press Oxford ; New York, 1987.

[20] R. Schrittwieser, C. Ionitá, J. Adámek, J. Stöckel, J. Brotánková, E. Martines, G. Popa, C. Costin, L. van de Peppel, and G. van Oost. Direct measurements of the plasma potential by katsumata-type probes. *Czechoslovak Journal of Physics*, 56(2):B145–B150, 2006.

[21] J Adamek, J Seidl, R Panek, M Komm, P Vondracek, J Stöckel, et al. Fast measurements of the electron temperature in divertor region of the compass tokamak using ball-pen probe.

[22] Stöckel J. M. Tichy G. Van Oost J. Adámek, C. Ionita R. Schrittwieser. Direct measurements of the electron temperature by a ball-pen/langmuir probe. *32nd EPS Conference on Plasma Phys*, 29, 2005.

[23] P C Stangeby. Determination of t e from a langmuir probe in a magnetic field by directly measuring the probe's sheath drop using a pin-plate probe. *Plasma Physics and Controlled Fusion*, 37(11):1337, 1995.